# Design of random laser and feature verification of FDTD software with the infrared wavelengths

Zhang Weijie[1], Song Kaishan[2]

(1. School of Computer Science and Engineering, Jilin Jianzhu University, Changchun 130033, China;
2. Northeast Institute of Geography and Agroecology, Chinese Academy of Sciences, Changchun 130033, China)

**Abstract:** An in-depth study of the localization properties of a random laser cavity is equivalent to the introduction of the theoretical analysis rate equation under external optical feedback lasers designed for magnetic optical crystal isolation devices to achieve improved random lasers. Using Nd:YAG laser, experimental results demonstrate that improved laser scattering loss can be reduced to achieve directional UV laser output. Finite-difference time-domain simulation results further show that the TE mode waveguide optical gain is approximately twice the planar waveguide, the coupled signal and pump intensity in improving the guide structure is significantly improved, and the output power results confirm the structure to reduce random laser scattering losses. Results of the application of random laser have an obvious reference value.

**Key words:** random laser; FDTD software; infrared wavelengths

**CLC number**: O23 **Document code**: A **DOI**: 10.3788/IRLA201645.1105006

# 红外波长的随机激光器设计及 FDTD 软件特性验证

张伟杰[1],宋开山[2]

(1. 吉林建筑大学 计算机科学与工程学院,吉林 长春 130033;
2. 中国科学院东北地理与农业生态研究所,吉林 长春 130033)

**摘 要**:深入研究了随机激光等效腔的局域化特性,引入了外部光反馈下激光器的理论分析速率方程,设计了磁旋光晶体的光隔离器件实现随机激光器的改进。采用的 Nd:YAG 激光器的实验结果验证了改进激光器可以降低散射损耗,实现紫外激光的方向性输出。FDTD 仿真结果进一步表明波导的 TE 模的光增益近似是平面波导的两倍;信号和泵浦强度的耦合在改进波导结构有了明显改进;输出功率结果证实了结构降低随机激光器的散射损耗。研究结果对于随机激光的应用具有明显的参考价值。

**关键词**:随机激光器; FDTD 软件; 红外波长

**收稿日期**:2016-03-17; **修订日期**:2016-04-23

**基金项目**:国家自然科学基金(41471290)

**作者简介**:张伟杰(1975-),女,副教授,硕士,主要从事光纤通信方面的研究。Email: zhangweijie902@163.com

## 0 Introduction

The advent of laser output instability was in the early 1960s, when the first laser was discovered [1]. However, this phenomenon received attention only in the 1970s and 1980s. In 1975, the Hake and Maxwell-Bloch equations and coordinate transformation [2-3], the nonlinear coupled equations describing a homogeneously broadened single-mode semiconductor laser into atmospheric convection in the Lorenz model, predict that it will have a chaotic phenomenon [4-7]. In 1985 [8], Weiso and others first discovered and confirmed the Haken-Lorenz chaos in an $NH_3$ laser after further studying many properties of laser chaos [9-10]. In 1985, Casperson observed the inhomogeneous broadening in the Xe laser self-pulsation mode splitting due to instability and explained this phenomenon using the Maxwell-Bloch semiclassical equation model [11-12]. The current random laser theory has proven random laser medium by random amplified quasi-state mold formation [13]. The refractive index of the medium in a strong random variation leads to localized waves that form a quasi-state mode [14]. The equivalent medium that forms a plurality of cavities can be called quasi-state equivalent optical cavity structure [15]. This equivalent optical cavity structure is analogous to the traditional optical cavity and can also support wave mode. If the threshold is exceeded and an access to the media after randomization is obtained, these quasi-state modes can be excited for the laser mode [16]. The optical waveguide structure is an effective way to limit and control the propagation of light. This idea has been expanded to enhance the random medium laser characteristics. A task force against the above-mentioned condition, an in-depth study of the localization properties of random laser equivalent cavity, improved the structure because the application of the results of the random laser has an obvious reference value.

## 1 Laser structure design

### 1.1 Dynamic characteristics

Figure 1 is a schematic of the reflection end

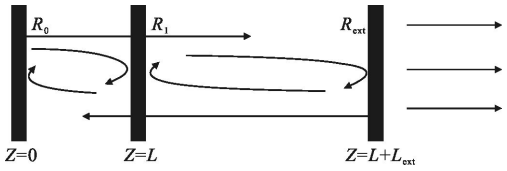


Fig.1 Schematic of the optical feedback

surfaces of the laser resonator optical feedback $R_0$ and $R_1$, the cavity length $L$, and the reflectance of the external mirror. The main physical processes of a laser include a carrier confinement mechanism, an optical waveguide process, and a photoelectric conversion process. The equations of Lang and Kobayashi are used to describe the laser carrier concentration as a result of the fluctuations in the photon density; these fluctuations make the prediction of each change between them difficult. Random lasers can also use the dynamic characteristics of the included feedback items (including EEL and VCSEL).

$$\frac{\mathrm{d}S(t)}{\mathrm{d}t}=\frac{G_0(N(t)-N_0)S(t)}{1+\varepsilon S(t)}-\frac{S(t)}{\tau_P}+2\frac{k_c}{\tau_L}\sqrt{S(t)\cdot S(t-\tau)}\cos(\theta(t))+F_S(t) \tag{1}$$

$$\frac{\mathrm{d}\phi(t)}{\mathrm{d}t}=\frac{\alpha G_0(N(t)-N_{\mathrm{th}})}{2}-\frac{k_c}{\tau_L}\sqrt{S(t-\tau)/S(t)}\sin(\theta(t))+F_\phi(t) \tag{2}$$

$$\frac{\mathrm{d}N(t)}{\mathrm{d}t}=\frac{I}{q}-\frac{G_0(N(t)-N_0)S(t)}{1+\varepsilon S(t)}-\frac{N(t)}{\tau_N}+F_N(t) \tag{3}$$

Equation (1) is the photon density rate equation, Eq. (2) is the phase equation, and Eq. (3) is the inverted carrier density equation. $F_S(t)$, $F_\phi(t)$, $F_N(t)$ is the Langevin noise term. The change of the laser phase is calculated as $\theta(t)=\frac{2\pi}{\lambda}\tau+\phi(t)-\phi(t-\tau)$, where $\tau$ is an optical external cavity round-trip delay time. The material gain is calculated as $G_0=\Gamma g_n v_g/V$. Feedback parameters, $k_c=(1-R_{\mathrm{DBR}})\sqrt{R_{\mathrm{ext}}/R_{\mathrm{DBR}}}$, represent the ratio of the return light within the electric field amplitude at the output end face of the reflected light to measure the intensity of the feedback light. $R_{\mathrm{DBR}}$ is the DBR reflectivity and $R_{\mathrm{ext}}$ is the intensity of the external cavity mirror reflectivity. Hence, the feedback

strength is calculated as $r$=10log ($k_c^2$). For the VCSEL microcavity structure, the dimensions of the active area are typically less than the diffusion length. The concentration of carriers in the active region does not change, and the external optical feedback of the carrier does not have a substantial effect. The diffusion can be neglected items and feedback items; hence, the carrier concentration of the rate equation includes carriers and carrier injection rate caused by a variety of complex losses. Therefore, the external optical feedback is reflected in the rate equation of the density equation and phase equations.

### 1.2 Optical isolation device design

To prevent the stability of the external feedback light into the laser, we used the laser output damage impact "laser curtain speed system" detection accuracy. We placed an optical isolator between the collimator lens and the beam expander, and a laser, collimator lenses, beam expanders, and an integrated optical isolator (Fig.2). For this purpose, we use a high Verdet constant magnetic optical crystal.

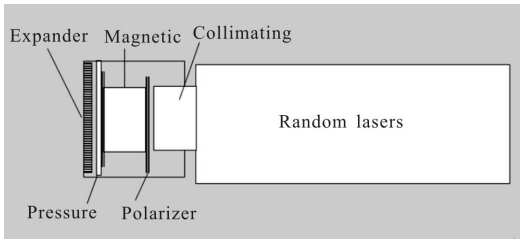


Fig.2 Schematic of the laser structure

The introduction of any optical element inevitably brings some passive components with inherent negative impact on the optical system, such as increase in insertion loss, increase in polarization mode dispersion in the system, increase in polarization-dependent loss, and increase in the difficulty of integrated optical systems. Only the strong optical feedback laser output was likely to produce chaos. In this study, the use of ZnO thin films can be enhanced within the lateral limit of light, thereby significantly improving the optical gain of ZnO thin films. Figure 3 shows a schematic of a random ZnO waveguide lasers. The particulate material consists of random media, and the spatial distribution of the particles is not uniform. The distribution of the scattering particles is greater in some areas. A relatively stronger light wave generating multiple scattering (in which photons prolonged residence time, resulting in waves localized states) played a role in the optical cavity so that the random medium at the pump can produce excitation laser oscillation.

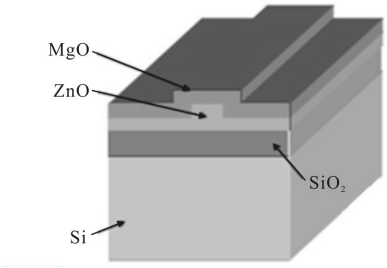


Fig.3 Schematic of ZnO random lasers

## 2 Experimental system design

As shown in Fig.4, the room, with a the third-harmonic Nd:YAG laser at 10 ns, a pulse at 12 Hz, a sample pump wavelength of 360 nm, and a beam diameter of approximately 25, is incident along a defined direction to the test sample. Laser radiation is

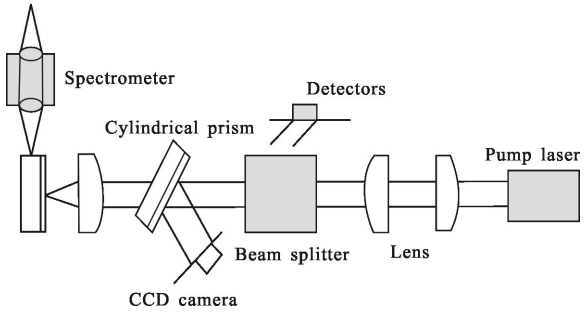


Fig.4 ZnO random laser ridge waveguide structure design

received through the cylindrical lens with CCD images, but through a collimating lens, with a spectrometer to detect. Figure 5 shows the diagram of the far-field emission in the pump intensity 1.4 MW/cm and a TE mode with and without epitaxial MgO layer.

The light does not exit the surface of the sample, which has a MgO buffer layer, showing a more circular spot. In contrast, the sample displayed an improved structure of a single spot emission. Therefore, the description of the waveguide laser with an improved random structure can be improved to reduce scattering losses and achieve directional UV laser output.

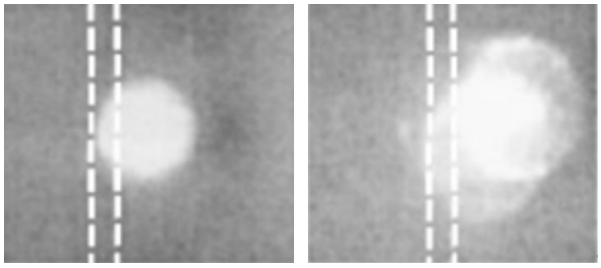

(a) Unimproved structure (b) Improved structure

Fig.5 Far-field emission of TE mode

## 3 Finite-difference time-domain simulation results

The principle of finite-difference time-domain (FDTD) simulation is based on modeling and studies of light propagation in different optical structures: the specific analog equivalent waveguide random lasers, the optical cavity mode, the background structure of the vacuum chamber, the 360 nm free-space wavelength, and the 2.5 m cavity length in the area around the microcavity using lattice grid points as a ridge PML absorbing a 5 000 boundary to terminate the computational domain. In the PML, the selected grid point $x$ is the distance from the boundary layer PML, and $z$ is the thickness of the layer PML. The spacing of the core region and the absorbing layer is calculated as $\Delta_{interval}$=1.4 μm. Spatial step is calculated as $\Delta x$=$\Delta z$=0.01 μm. The simulation results are shown in Eq.6. To further analyze the advantages of a waveguide structure, we used the case of the planar waveguide for comparison and analysis of the problem of optical loss. For the field distribution in the case, some data can be obtained. The value is calculated under the same excitation power, and the gain of the TE mode optical waveguide is approximately twice the plane. The coupling signal and the pump intensity ridge waveguide structure enhanced significantly. Figure 6 is the laser electric field distribution. Figure 7 shows the improved structure of the TE mode and the planar waveguide optical gain and a chart comparing the relationship between the intensity of the pump.

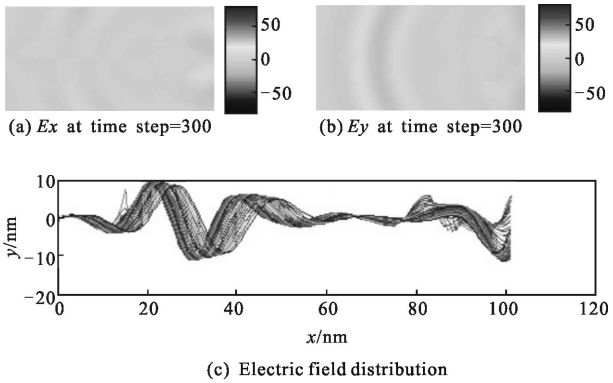


(c) Electric field distribution

Fig.6 Laser electric field distribution

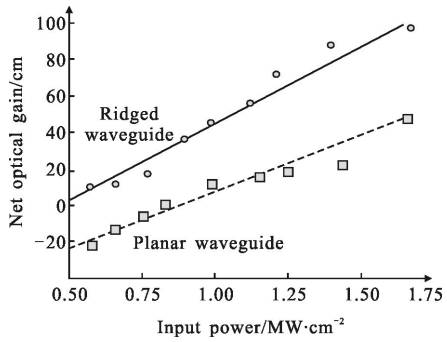


Fig.7 Net optical gain and pump intensity diagram

In the improved sample threshold pump structure (output power), it is confirmed that the sample reduces random scattering losses of the laser. The pump intensity at 1.4 MW/cm$^2$ improves the characteristics of the sample and laser TE mode common structure, as shown in Fig.8. A folding point at both 0.63 MW/cm and 0.71 MW/cm$^2$ (at the threshold) can be seen when the pump intensity is higher than the folding point (Fig.8). It can be observed that the line is less than the peak value of 0.4 nm (laser mode), and when the pump intensity is further increased, the peak in

the spectrum more appears. As the excitation peak increases, the number of areas increases. Thus, an epitaxial layer of ZnO is verified with the (200)–oriented ZnO to produce a coherent random laser. The coherent backscattering experiments show that considerable time with the (200)–oriented ZnO scattering mean free path of the epitaxial layer and the emission wavelength will produce coherent random laser.

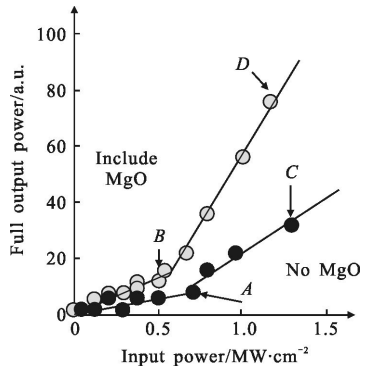


Fig.8 Laser characteristic samples in TE mode

## 4 Conclusion

This paper design the magnetic optical crystal optical isolation devices to achieve improved random lasers. Using Nd:YAG laser, the experimental results demonstrate that laser scattering loss can be reduced to achieve directional UV laser output. By the FDTD method simulation, numerical simulation results demonstrate that improved ZnO waveguide random lasers can achieve a high degree of orientation of the outgoing characteristics, which is also avoiding nonaxial laser emission and can significantly reduce the scattering loss.

### References:

[1] Meng X, Fujita K, Murai S, et al. Coherent random lasers in weakly scattering polymer films containing silver nanoparticles[J]. ***Physical Review A***, 2009, 79(5): 1744–1747.

[2] Jonathan Andreasen, Nicolas Bachelard, Shivakiran B N, et al. Partially pumped random lasers[J]. ***International Journal of Modern Physics B***, 2014, 28(5): 208–210.

[3] Leonetti Marco, Conti Claudio, Lopez Cefe. The mode-locking transition of random lasers [J]. ***Nature Photonics***, 2013, 5(10): 615–617.

[4] Zhu Jun, Li Zhiquan, Qin Liuli. Cavity physical properties of SPP propagation in the MIM structure [J]. ***Infrared and Laser Engineering***, 2015, 42(3): 852–856.

[5] Oleg Zaitsev, Lev Deych. Recent developments in the theory of multimode random lasers[J]. ***Journal of Optics***, 2009, 12 (2) 150–152.

[6] Hutchings M, O′Driscoll I, Smowton P M, et al. Fermi-dirac and random carrier distributions in quantum dot lasers [J]. ***Applied Physics Letters***, 2014, 104(3): 031103.

[7] Zhu Jun, Qin Liuli, Song Shuxiang, et al. Design of a surface plasmon resonance sensor based on grating connection [J]. ***Photonic Sensors***, 2015, 5(2): 159–165.

[8] Hoefner M, Wuensche H, Henneberger F. A random laser as a dynamical network [J]. ***New Journal of Physics***, 2014, 16(3): 245–248.

[9] Zhu Jun, Qin Liuli, Song Shuxiang. Surface plasmon resonance demodulation by optical ring-down cavity technology [J]. ***Optik-International Journal for Light and Electron Optics***, 2015, 4026(3): 201.

[10] Andreasen J, Cao H. Spectral behavior of partially pumped weakly scattering random lasers[J]. ***Optics Express***, 2011, 19 (4): 3418–3433.

[11] Shen Z, Wu L, Zhu S, et al. Random lasing action in a polydimethylsiloxane wrinkle induced disordered structure[J]. ***Applied Physics Letters***, 2014, 105(2): 021106.

[12] Ye L, Liu B, Zhao C, et al. The electrically and magnetically controllable random laser from dye-doped liquid crystals[J]. ***Journal of Applied Physics***, 2014, 116(5): 053103.

[13] Leonetti M, Conti, C, Lopez C. Tunable degree of localization in random lasers with controlled interaction [J]. ***Applied Physics Letters***, 2012, 101(5): 051104.

[14] Geng J, Wang Q, Lee Y, et al. Development of eye-safe fiber lasers near 2 μm [J]. ***IEEE Journal of Selected Topics in Quantum Electronics***, 2014, 20(5): 150–160.

[15] Feng L, Li P, Zhang M, et al. Transition linewidth of cross correlations in random intensity fluctuations in electromagnetically induced transparency [J]. ***Physical Review A***, 2014, 89(1): 267–274.

[16] Krämmer Sarah, Vannahme Christoph, Smith Cameron L, et al. Random-cavity lasing from electrospun polymer fiber networks [J]. ***Advanced Materials***, 2014, 26(48): 8096–8100.